

# Unifying local and global model explanations by functional decomposition of low dimensional structures

Munir Hiabu <sup>\*1</sup>, Joseph T. Meyer<sup>2</sup>, and Marvin N. Wright<sup>3,4,5</sup>

<sup>1</sup>Department of Mathematical Sciences, University of Copenhagen,  
2100 Copenhagen O, Denmark

<sup>2</sup>Institute for Applied Mathematics, Heidelberg University, Im  
Neuenheimer Feld 205, 69120 Heidelberg, Germany

<sup>3</sup>Leibniz Institute for Prevention Research & Epidemiology – BIPS,  
Bremen, Germany

<sup>4</sup>Faculty of Mathematics and Computer Science, University of  
Bremen, Bremen, Germany

<sup>5</sup>Department of Public Health, University of Copenhagen,  
Copenhagen, Denmark

August 15, 2022

## Abstract

We consider a global explanation of a regression or classification function by decomposing it into the sum of main components and interaction components of arbitrary order. When adding an identification constraint that is motivated by a causal interpretation, we find  $q$ -interaction SHAP to be the unique solution to that constraint. Here,  $q$  denotes the highest order of interaction present in the decomposition. Our result provides a new perspective on SHAP values with various practical and theoretical implications: If SHAP values are decomposed into main and all interaction effects, they provide a global explanation with causal interpretation. In principle, the decomposition can be applied to any machine learning model. However, since the number of possible interactions grows exponentially with the number of features, exact calculation is only feasible for methods that fit low dimensional structures or ensembles of those. We provide an algorithm and efficient implementation for gradient boosted trees (xgboost)<sup>1</sup> and random planted forests that calculates this decomposition. Conducted

---

<sup>\*</sup>mh@math.ku.dk (Corresponding author)

<sup>1</sup><https://github.com/PlantedML/glex>

experiments suggest that our method provides meaningful explanations and reveals interactions of higher orders. We also investigate further potential of our new insights by utilizing the global explanation for motivating a new measure of feature importance, and for reducing direct and indirect bias by post-hoc component removal.

## 1 Introduction

In the early years of machine learning interpretability research, the focus was mostly on global feature importance methods that assign a single importance value to each feature. More recently, the attention has shifted towards local interpretability methods, which provide explanations for individual observations. Popular examples of the latter are LIME (Ribeiro et al., 2016) and SHAP (Shapley, 1953; Lipovetsky and Conklin, 2001; Lundberg and Lee, 2017). The major reason for this shift is that local methods provide a more comprehensive picture of model explanations than single-value global methods, most importantly in presence of nonlinear effects and interactions. This, however, neglects the fact that global methods can be more than single-value methods: Ideally, a global method provides useful information about the entire regression or classification function by providing an explanation for each feature and each interaction effect of arbitrary order, relative to the values they take. As with local methods, this gives us an explanation for each observation. The crucial difference is that two observations which have a set of features in common receive the same explanation for main effects and interaction effects involving exclusively those features. The reason is that higher order effects are not hidden in the main effects. A global explanation is not specific to observations but only to feature values, and it does not only give a more comprehensive picture than local methods but the complete picture.

In this paper, we introduce a global explanation procedure by identifying components in a functional decomposition. We show that the proposed global explanation is identical to  $q$ -interaction SHAP (Tsai et al., 2022), where  $q$  corresponds to the maximal order of interaction present in the model to be analyzed. Hence, we provide a new interpretation of SHAP values which is not game-theoretically motivated. We develop a fast implementation that exactly calculates  $q$ -interaction-SHAP for tree-based machine learning models. In principle, our results can be applied to any model and our algorithm can be applied to any tree-based model. However, since the number of components grows exponentially with increasing  $q$ , exact calculation is only feasible if  $q$  is sufficiently small, as e.g. in gradient boosted trees. We provide an implementation for *xgboost* (Chen and Guestrin, 2016) and *random planted forest* (Hiabu et al., 2020).

The  $q$ -interaction SHAP is a global explanation of a trained model. One and two-dimensional components can be plotted and together with higher order components they can be used to decompose local SHAP values into main effects and all involved interaction effects. Additionally, main and interaction components can be summarized into feature importance values. Beyond explaining feature

effects, our proposed decomposition can be used to detect bias in models where LIME and SHAP fail (Slack et al., 2020) and reduce such bias by removing individual components from the decomposition.

## 1.1 Motivating example

We will give a toy example of how the interplay of correlations and interactions can give rise to misleading SHAP values. Consider the function  $m(x_1, x_2) = x_1 + x_2 + 2x_1x_2$ . The SHAP value for the first variable is  $\phi_1(x_1, x_2) = x_1 - E[X_1] + x_1x_2 - E[X_1X_2] + x_1E[X_2] - x_2E[X_1]$ . If the features are standardized, i.e.,  $X_1$  and  $X_2$  have mean zero and variance one, the expression reduces to

$$\phi_1(x_1, x_2) = x_1 + x_1x_2 - \text{corr}(X_1, X_2).$$

Hence, e.g., if  $\text{corr}(X_1, X_2) = 0.3$ , an individual with  $x_1 = 1$  and  $x_2 = -0.7$  would see a SHAP value of 0 for the first variable:

$$\phi_1(1, -0.7) = 0.$$

This is quite misleading, since clearly  $x_1$  has an effect on the response  $m$  that is irrespective of the particular value of  $x_1$ . The underlying problem is that locally at  $(x_1, x_2) = (1, -0.7)$ , the main effect contribution and interaction contribution cancel each other out. Indeed, we will see that the SHAP value  $\phi_1$  can be decomposed into a main effect contribution of  $\{x_1\}$ , which is  $x_1 - 2\text{corr}(X_1, X_2) = 0.4$  and an interaction contribution of  $\{x_1, x_2\}$ , which is  $x_1x_2 + \text{corr}(X_1, X_2) = -0.4$ . Figure 1 shows SHAP values and the functional decomposition of an *xgboost* model of the function  $m(x_1, x_2)$ . The SHAP values  $\phi_1$  and  $\phi_2$  contain main effect contributions  $m_1$  and  $m_2$  as well as the interaction contribution  $m_{12}$ . The functional decomposition separates the contributions  $m_1$ ,  $m_2$  and  $m_{12}$ .

Those familiar with SHAP values may argue that one can detect the non-zero impact of  $x_1$  by plotting  $\phi_1$  over all instances (see Figure 1). This argument has two problems. Firstly, this does not change the misleading local value. Secondly, SHAP values can be quite arbitrary: Two estimators that are equal on the support of the data can have very different SHAP values. To see this, define  $\tilde{m}(x) = m(x) + \alpha(x)$ , where  $\alpha(x) = 0$ , for  $x \in \text{supp}(X_1, X_2)$ , and choose  $\alpha$  outside the support of  $(X_1, X_2)$  such that it approximates some desired SHAP values. This works because SHAP values are constructed by extrapolating outside the support of the data. Slack et al. (2020) has empirically demonstrated how this can be exploited to hide the importance of protected features. One could ask for local explanations that do not extrapolate, hoping that this solves the problem. Unfortunately, this is not the case: If explanations are deduced only from the region with data support, those explanations are based on the correlation structure of the features (Janzing et al., 2020). In particular a variable that has zero effect on the model output can still be assigned a value stemming from a correlated variable (Janzing et al., 2020; Sundararajan and Najmi, 2020). We conclude:

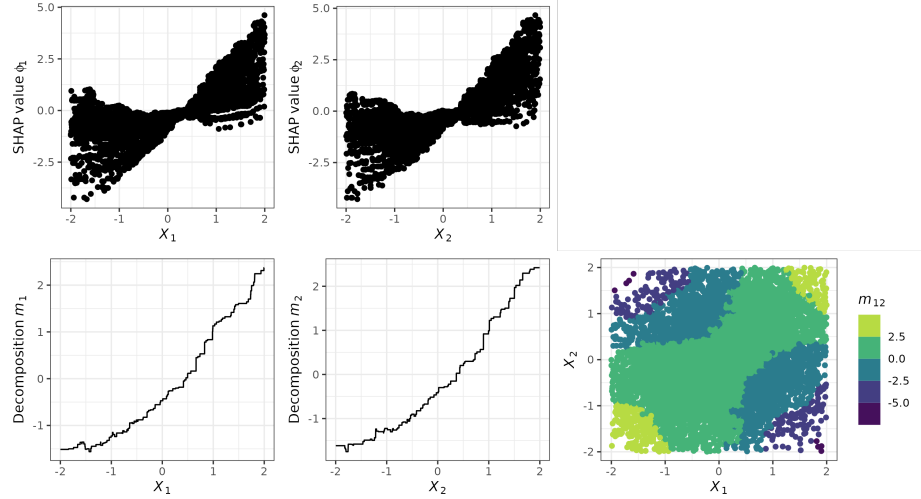


Figure 1: Simple example. SHAP values (top row) and functional decomposition (bottom row) of an *xgboost* model of the function  $m(x_1, x_2) = x_1 + x_2 + 2x_1x_2$ .

*Local explanations that do not explicitly specify all interactions cannot lead to meaningful causal interpretations in the presence of correlated features.*

This is worrying noting that interpretation tools are usually used for black-box algorithms with the main purpose being to explain the model well in cases where interactions are present. A local interpretation that considers all interactions is actually a global interpretation. Hence the goal of this paper is to unify local and global explanations.

## 1.2 Related Work

A functional decomposition for global interpretation of regression functions was introduced in the statistical literature in Stone (1994), and has been further discussed in Hooker (2007); Chastaing et al. (2012); Lengerich et al. (2020). These authors considered a different constraint called (generalized) functional ANOVA decomposition. In contrast, the constraint we introduce in this paper is linked to Shapley values. There is considerable literature on interactions and Shapley values. In cooperative game theory, pairwise player-player interactions were first considered by Owen (1972) and later generalized to higher-order interactions by Grabisch and Roubens (1999). In the machine learning context, arbitrariness of Shapley values due to interactions and correlations has been discussed in Kumar et al. (2020), Slack et al. (2020), Sundararajan and Najmi (2020), and possible solutions have been proposed in Zhang et al. (2021), Kumar et al. (2021), Harris et al. (2022), Ittner et al. (2021), Sundararajan et al. (2020). Recently, Tsai et al. (2022) introduced interaction SHAP for any given

order and proposed an approximation to calculate them. In this paper, we introduce an identification constraint for a functional decomposition that is motivated by a causal interpretation, which will connect to Shapley values with a value function that has recently been coined interventional SHAP (Chen et al., 2020). Alternative value functions have been discussed in Frye et al. (2020), Yeh et al. (2022). There are a variety of methods to obtain global feature importance measures implied by SHAP, in the form of a single value. These include Casalicchio et al. (2018), Frye et al. (2020) and Williamson and Feng (2020), among others. Similar to our method suggested in Section 3, the measures are obtained by weighted averages of local importance values. However, in contrast to our suggestion, most are motivated by additive importance measures (Covert et al., 2020).

## 2 Main result

Let  $(Y_i, X_{i,1}, \dots, X_{i,d})$  be a data set of  $n$  i.i.d. observations with  $X_{i,k} \in \mathbb{R}$ ,  $i = 1, \dots, n$ ;  $k = 1, \dots, d$ . We consider the supervised learning setting

$$E[Y_i|X_i = x] = m(x),$$

where the function  $m$  is of interest and  $Y$  is a real valued random variable.<sup>2</sup> We assume that a reasonable estimator  $\hat{m}$  of  $m$  has been provided.

### 2.1 Global Interpretation

With increasing dimension it can quickly get very hard, if not impossible, to visualize and thereby comprehend a multivariate function. Hence, a global interpretation of  $\hat{m}$  is arguably only feasible if it is a composition of low-dimensional structures. Let us consider a specific decomposition of a multivariate function into a sum of main effects, bivariate interactions, etc., up to a  $d$ -variate interaction term.

$$\hat{m}(x) = \hat{m}_0 + \sum_{k=1}^d \hat{m}_k(x_k) + \sum_{k < l} \hat{m}_{kl}(x_k, x_l) + \dots + \hat{m}_{1,\dots,d}(x) = \sum_{S \subseteq \{1, \dots, d\}} \hat{m}_S(x_S). \quad (1)$$

The heuristic of the decomposition is that if the underlying function  $m(x)$  only lives on low-dimensional structures, then  $m_S$  should be zero for most feature subsets  $S$  and the order of maximal interaction  $q = \max\{|S| : m_S \neq 0\}$  should be much smaller than the number of features:  $q \ll d$ . This discussion, however, is not very meaningful before one has agreed on an identification; without suitable identification constraints, it is possible to change components on the right without altering the left hand side. We propose the following identification:

---

<sup>2</sup>We use  $Y_i \in \mathbb{R}$  for national convenience. It is straight-forward to extend to binary classification, whereas multiclass classification would require a slightly different procedure.

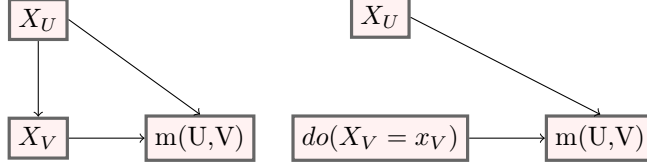


Figure 2: Left: Initial causal structure. Right: Causal Structure after removing effect of  $X_U$  on  $X_V$ .

**Marginal identification:** For every  $S \subseteq \{1, \dots, d\}$ ,

$$\sum_{T \cap S \neq \emptyset} \int \hat{m}_T(x_T) \hat{p}_S(x_S) dx_S = 0, \quad (2)$$

where  $\hat{p}_S$  is some estimator of the density  $p_S$  of  $X_S$ . The identification can be motivated by a causal interpretation.

Assume  $U$  is a set of features that should not have an effect on  $\hat{m}$ . For example  $U = \{\text{gender, ethnicity}\}$  in the case of non-discriminatory regulation requirements. Assume  $\{1, \dots, d\}$  is the disjoint union of  $U$  and  $V$  with a directed acyclic graph structure  $X_U \rightarrow X_V \rightarrow m$ ,  $X_U \rightarrow m$ ; as illustrated in Figure 2. Eliminating the causal relationship between  $X_V$  and  $X_U$  can be achieved via the do-operator,  $do(X_V = x_V)$ , that removes all edges going into  $X_V$ , see Figure 2. The function  $E[m(X) | do(X_V = x_V)]$  does not use information contained in  $X_U$ ; neither directly nor indirectly. Under the assumed causal structure, standard calculations (Pearl, 2009) lead to

$$E[m(X) | do(X_V = x_V)] = \int m(x) p_U(x_U) dx_U.$$

If  $\hat{m}$  is identified via (2), then  $\tilde{m}(x_{-U}) := \int \hat{m}(x) \hat{p}_U(x_U) dx_U$  can be extracted from  $\hat{m}$  by dropping all components that include variables in  $U$ :

$$\tilde{m}(x_{-U}) = \int \hat{m}(x) \hat{p}_U(x_U) dx_U = \sum_{S \subseteq V} \hat{m}_S(x_S).$$

The next theorem states existence and uniqueness of a decomposition that satisfies the identification constraint (2) and describes the solution explicitly.

**Theorem 2.1.** Given any initial estimator  $\hat{m}^{(0)} = \{\hat{m}_S^{(0)} | S \subseteq \{1, \dots, d\}\}$ , there exists exactly one set of functions  $\hat{m}^* = \{\hat{m}_S^* | S \subseteq \{1, \dots, d\}\}$  satisfying constraint (2) with  $\sum_S \hat{m}_S^* = \sum_S \hat{m}_S^{(0)}$ . The functions are given by

$$\hat{m}_S^*(x_S) = \sum_{T \supseteq S} \sum_{T \setminus S \subseteq U \subseteq T} (-1)^{|S| - |T \setminus U|} \int \hat{m}_T^{(0)}(x_T) \hat{p}_U(x_U) dx_U. \quad (3)$$

In particular  $\hat{m}^*$  does not depend on the particular identification of  $\hat{m}^{(0)}$ .

**Example 2.2.** Going back to the setting of our simple example (Section 1.1),  $m(x_1, x_2) = x_1 + x_2 + 2x_1x_2$ , we have

$$m(x_1, x_2) = m_0^* + m_1^*(x_1) + m_2^*(x_2) + m_{12}^*(x_1, x_2),$$

where  $m_0^* = c = 2\text{corr}(X_1, X_2)$ ,  $m_1^*(x_1) = x_1 - c$ ,  $m_2^*(x_2) = x_2 - c$ ,  $m_{12}^*(x_1, x_2) = 2x_1x_2 + c$ .

In principle, in Theorem 2.1 we could always consider  $\hat{m}_{\{1, \dots, d\}}^{(0)} = \hat{m}^{(0)}$  and  $\hat{m}_S^{(0)} = 0$  otherwise as an initial estimator. This would simplify the notation. In Section D, we will discuss that if  $\hat{m}^{(0)}$  is a composition of low dimensional structures, then  $\hat{m}^*$  can be calculated reasonably fast. In this case, we exploit the fact that  $\hat{m}^{(0)}$  can be represented by functions  $\hat{m}_S^{(0)}$ , where  $\hat{m}_S^{(0)} = 0$  for  $|S| \geq q < d$ , which is why the more complicated notation is used. We provide an implementation for *xgboost* (Chen and Guestrin, 2016) and *random planted forest* (Hiabu et al., 2020).

## 2.2 From global to local explanation

Fix a value  $x_0 \in \mathbb{R}^d$ . A local approximation of the function  $\hat{m}$  is given by

$$\hat{m}(x_0) = \phi_0 + \sum_{k=1}^d \phi_k(x_0), \quad (4)$$

for constants  $\phi_0, \phi_1(x_0), \dots, \phi_d(x_0)$ . Similar to the case of global explanations, the right hand-side is not identified. Local explanations add constraints to equation (4) aiming for an identification such that  $\phi_k(x_0)$  reflects the local contribution of the variable  $X_k$  to  $\hat{m}(x_0)$ . Consider a value function  $v_{x_0}$  that assigns a real value  $v_{x_0}(S)$  to each subset  $S \subseteq \{1, \dots, d\}$ . Shapley axioms provide a unique solution under the four axioms efficiency, symmetry, dummy and additivity (Shapley, 1953), see Section A in the appendix. Defining  $\Delta_v(k, S) = v(S \cup k) - v(S)$ , the Shapley values are

$$\phi_k = \frac{1}{d!} \sum_{\pi \in \Pi_d} \Delta_v(k, \{\pi(1), \dots, \pi(k-1)\}) = \frac{1}{d!} \sum_{S \subseteq \{1, \dots, d\} \setminus \{k\}} |S|!(d-|S|-1)! \Delta_v(k, S), \quad (5)$$

where  $\Pi_d$  is the set of permutations of  $\{1, \dots, d\}$ . We follow (Janzing et al., 2020) and define SHAP values as Shapley values with the value function

$$v_{x_0}(S) = \int \hat{m}(x) \hat{p}_{-S}(x_{-S}) dx_{-S} |_{x=x_0}, \quad (6)$$

which is also the version implemented in TreeSHAP (Lundberg et al., 2020).

We show that there is a direct connection between the global explanation described in the previous section and SHAP values defined via (6). In particular, this connection describes SHAP values uniquely without the use of the Shapley

axioms or formula (5), running through permutations, where the number of summands grows exponentially with  $d$ . The result is intriguing since usually the contribution or importance of a single variable in a general global representation as in (1) is a complicated interplay between various interactions, see Section C in the appendix.

**Corollary 2.3.** If  $\hat{m}$  is decomposed such that (2) is fulfilled, then the SHAP values are weighted averages of the corresponding components, where an interaction component is equally split to all involved variables:

$$\phi_k(x) = \hat{m}_k^*(x_k) + \frac{1}{2} \sum_j \hat{m}_{kj}^*(x_{kj}) + \cdots + \frac{1}{d} \hat{m}_{1,\dots,d}^*(x_{1,\dots,d}).$$

**Remark 2.4.** A crucial point of Corollary 2.3 is that the local SHAP values can be described by a composition of global explanations. By this we mean that while  $\phi_k(x)$  depends on all components of  $x$ , the function  $\hat{m}_S^*$  does not depend on values  $x_{\{1,\dots,d\} \setminus S}$ .

### 3 Feature importance

The global interpretation also provides a new perspective on feature importance. SHAP value feature importance for feature  $k$  is usually given by an empirical version of  $E[|\phi_k(x)|]$ . By Corollary 2.3,

$$E[|\phi_k(x)|] = E \left[ \left| \sum_{S:k \in S} \frac{1}{|S|} \hat{m}_S^*(x_S) \right| \right].$$

In this definition, contributions from various interactions and main effects can cancel each other out, which may not be desirable. An alternative is to consider

$$E \left[ \sum_{S:k \in S} \frac{1}{|S|} |\hat{m}_S^*(x_S)| \right]$$

or to extend the definition of variable importance to interactions by defining variable importance as  $E[|\hat{m}_S^*(x_S)|]$ , for a set  $S \subseteq \{1, \dots, d\}$ .

**Example 3.1.** Going back to our simple example (Section 1.1), where  $m(x_1, x_2) = x_1 + x_2 + 2x_1x_2$ , SHAP variable importance for variable  $x_1$  is an empirical version of

$$E \left[ \left| x_1 - 2\text{corr}(X_1, X_2) - \frac{1}{2} \{2x_1x_2 + 2\text{corr}(X_1, X_2)\} \right| \right] = E [|x_1 - x_1x_2 - \text{corr}(X_1, X_2)|],$$

which merges main effect and interaction effect. Alternatively, one may consider

$$E [|x_1 - 2\text{corr}(X_1, X_2)| + |x_1x_2 + \text{corr}(X_1, X_2)|].$$

## 4 Experiments

We apply our method to several real and simulated datasets to show that the functional decomposition provides additional insights compared to SHAP values and SHAP interaction values. First, we show on real data that a global explanation can provide a more comprehensive picture than a local explanation method. Second, we show on real and simulated data that the same holds for the feature importance measure proposed in Section 3. Finally, we show that the functional decomposition allows post-hoc removal of features from a model, which can be used to reduce bias of prediction models. We performed all experiments with *xgboost* and *random planted forests*. The results with *xgboost* are presented in Sections 4.1-4.3 in the main paper, whereas the results with *random planted forests* are in Sections E.1-E.3 in the appendix.

### 4.1 Global explanations

As an example of a real data application, we apply our method to the *bike sharing* data (Fanaee-T and Gama, 2014), predicting the number of rented bicycles per day, given seasonal and weather information. Figure 3 shows SHAP values, main effects, 2-way interactions and 3-way interactions of the features *hour of the day* (hr, 0-24 full hours), *Temperature* (temp, normalized to 0-1) and *working day* (workingday, 0=no, 1=yes). In the top row, we see that different SHAP values are observed for the same values of the features and conclude that SHAP values are not sufficient to describe the features' effects on the outcome, due to interactions. In the second row, the main effects from the decomposition show a strong effect of the hour of the day: Many bikes are rented in the typical commute times in the morning and afternoon. We also see a positive effect of the temperature and no main effect of whether or not it is a working day. The 2-way interactions in the third row reveal strong interactions between the hour of the day and working day: On working days, more bikes are rented in the morning and less during the night and around noon. We also see that the temperature has a slightly higher effect on non working days and in the afternoon. In the bottom row, the 3-way interactions show that interactions between the hour of the day and the temperature are stronger on non working days than on working days. We conclude that the full functional decomposition provides a more comprehensive picture of the features' effects, compared to usual SHAP value interpretations and 2-way interaction SHAP, as e.g. proposed by Lundberg et al. (2020). Note that, as described above, our methods do indeed provide the full picture, including all higher-order interactions, whereas Figure 3 only shows a subset of these interactions.

### 4.2 Feature importance

As described in Section 3, the functional decomposition can also be used to calculate feature importance. Figure 4 shows the feature importance for the function  $m(x) = x_1 + x_3 + x_2x_3 - 2x_2x_3x_4$  and the bike sharing data from

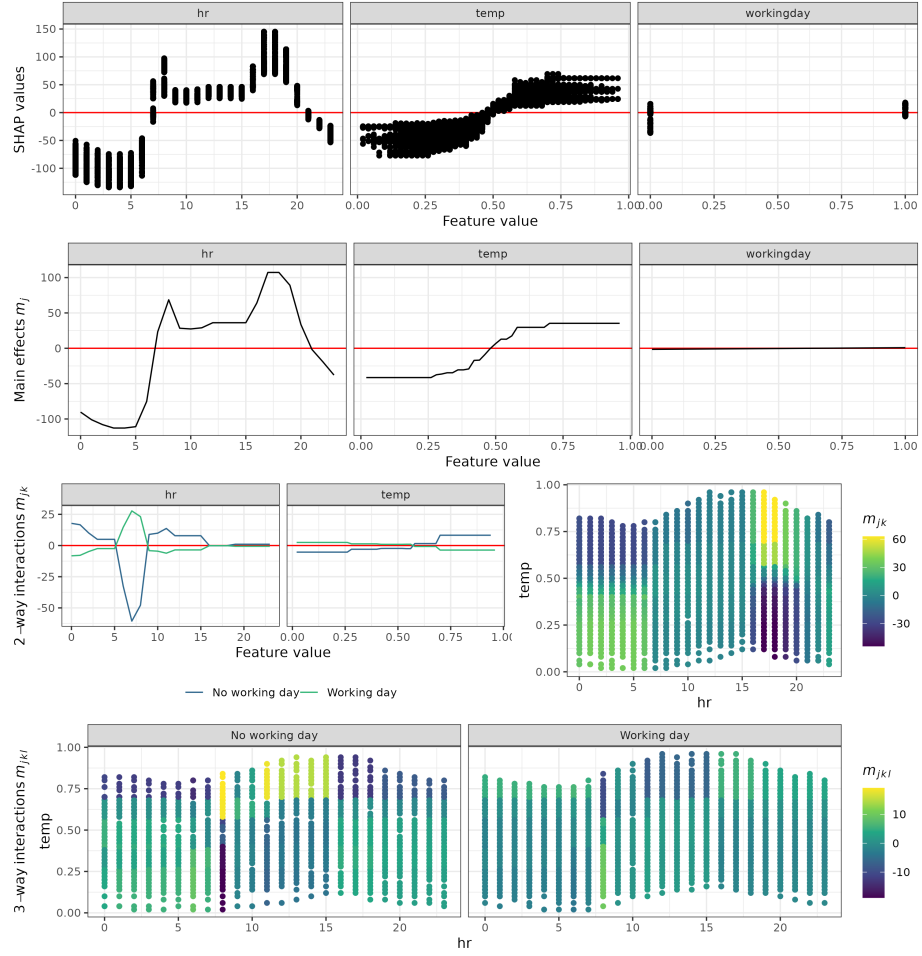


Figure 3: Bike sharing example (*xgboost*). SHAP values (top row), main effects (second row), 2-way interactions (third row) and 3-way interactions (bottom row) of the features *hour of the day* (*hr*, 0-24 full hours), *Temperature* (*temp*, normalized to 0-1) and *working day* (*workingday*, 0=no, 1=yes) of the bike sharing data.

Section 4.1 based on SHAP values and our functional decomposition. For the simple function, the SHAP feature importance identifies  $x_1$  and  $x_3$  as equally important and  $x_2$  and  $x_4$  as less important but it gives no information about interactions. On the other hand, the feature importance based on the functional decomposition shows that  $x_1$  has a strong main effect but no interactions, whereas  $x_2$  and  $x_4$  have only interaction effects but no main effects and  $x_3$  both kinds of effect. Similarly, on the bike sharing data, the hour of the day (feature  $hr$ ) and the temperature ( $temp$ ) have both main and interaction effects, whereas the feature *working day* has 2-way interaction effects but no main effects (compare Figure 3). Note that both definitions of feature importance are based on absolute values of SHAP values or components  $m_S$  and thus are non-negative, in contrast to other methods of feature importance (Nembrini et al., 2018; Casalicchio et al., 2018).

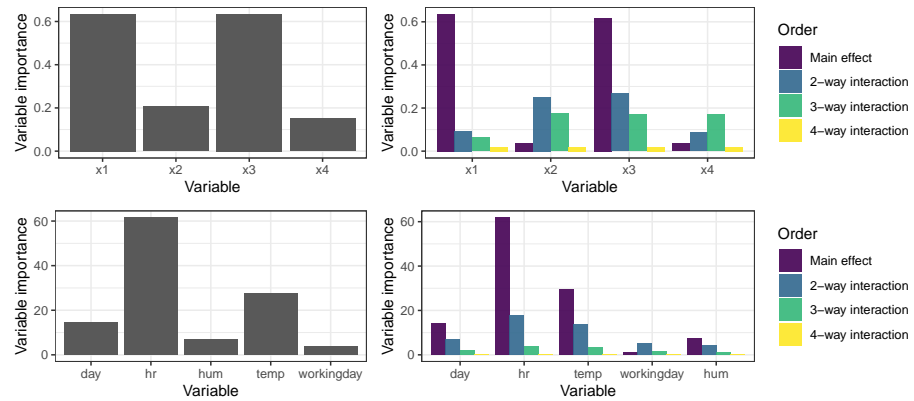


Figure 4: Feature importance (*xgboost*) for the function  $m(x) = x_1 + x_3 + x_2x_3 - 2x_2x_3x_4$  (top row) and the bike sharing data from Section 4.1 (bottom row) based on SHAP values (left column) and our functional decomposition separately for main effects and interactions of different orders (right column).

### 4.3 Post-hoc feature removal

We show that our method can be used to remove features and all their effects, including interactions, from a model *post-hoc*, i.e. after model fitting. We trained models on simulated data and the *adult* dataset (Dua and Graff, 2017). Both models contained a feature *sex* or *gender*, which is a protected attribute and should not have an effect in fair prediction models (Barocas et al., 2019). In the simulation, we considered the simplified scenario where we predict a person's salary, based on their sex and weekly working hours. We set the weekly working hours to an average of 40 for men and to 30 for women. Salary was simulated as 1 unit (e.g. thousand Euro per year) per weekly working hour and an additional 20 for males (see Figure 2). Thus, men earn more for working longer hours (on

average) and for being male per se. The first effect should be kept by a fair machine learning model, whereas the second effect is discriminating women. In the *adult* data, we have the same features *sex* and *hours* but we do not know the causal structure.

Figure 5 shows the prediction for females and males of the full model, a refitted model without the protected feature *sex* and a decomposed model where the feature *sex* was removed post-hoc. In the simulated data, we see that refitting the model does not change the predictions at all: Because of the high correlation between *sex* and *hours*, the effects of *sex* cannot be removed by not considering the feature in the model. Our decomposition on the other hand allows us to remove the (unwanted) direct effect of *sex* while keeping the (wanted) indirect effect through *hours*. On the *adult* data, we see a similar difference, but less pronounced.

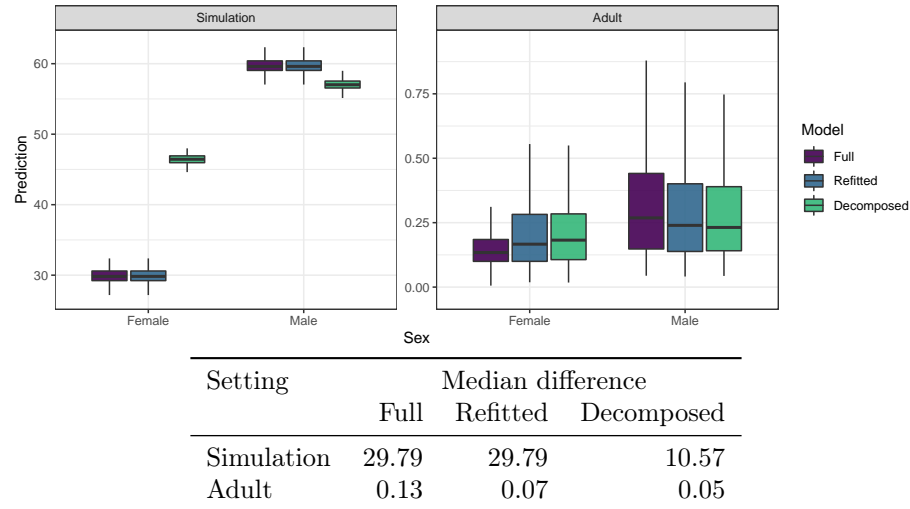


Figure 5: Post-hoc feature removal (*xgboost*). Predictions in a simulation (left) and the *adult* dataset for males and females of the full model, a refitted model without the protected feature *sex* and a decomposed model where the feature *sex* was removed post-hoc. The table below shows the median differences between females and males for the three models.

## 5 Concluding remarks and limitations

In this paper, we have introduced a way to turn local Shapley values into a global explanation using a functional decomposition. The global explanation has a causal interpretation under the DAG structure given in Figure 2. This causal structure might be quite realistic in many fairness considerations, but the true causal structure is generally unknown. In this respect, it would be

interesting to look into other causal structures that could motivate other identification constraints than (2), which may connect to other local explanations than interventional SHAP. Also, while our suggestions for variable importance measures paint a more precise picture in many cases, it is not directly motivated by a theoretical constraint, such as usual additive importance measures. It will require more research to back these ideas by theory. Another point not considered in this paper is the difference between the estimate  $\hat{m}$  and a potential true function  $m$ . In particular, it is not clear if a method that estimates  $m$  well is also a good estimator for a selection of components  $m_S$ . This discussion is related to work done in double/debiased machine learning (Chernozhukov et al., 2018). Moving forward, it could be interesting to modify out of the box machine learning algorithms to specifically learn the low dimensional structures well.

## References

Barocas, S., M. Hardt, and A. Narayanan (2019). *Fairness and Machine Learning*. <http://www.fairmlbook.org>.

Casalicchio, G., C. Molnar, and B. Bischl (2018). Visualizing the feature importance for black box models. In *Joint European Conference on Machine Learning and Knowledge Discovery in Databases*, pp. 655–670. Springer.

Chastaing, G., F. Gamboa, C. Prieur, et al. (2012). Generalized Hoeffding-Sobol decomposition for dependent variables-application to sensitivity analysis. *Electronic Journal of Statistics* 6, 2420–2448.

Chen, H., J. D. Janizek, S. Lundberg, and S.-I. Lee (2020). True to the model or true to the data? *arXiv preprint arXiv:2006.16234*.

Chen, T. and C. Guestrin (2016). Xgboost: A scalable tree boosting system. In *Proceedings of the 22nd ACM SIGKDD International Conference on Knowledge Discovery and Data Mining*, pp. 785–794.

Chernozhukov, V., D. Chetverikov, M. Demirer, E. Duflo, C. Hansen, W. Newey, and J. Robins (2018). Double/debiased machine learning for treatment and structural parameters. *The Econometrics Journal* 21(1), C1–C68.

Covert, I., S. M. Lundberg, and S.-I. Lee (2020). Understanding global feature contributions with additive importance measures. *Advances in Neural Information Processing Systems* 33, 17212–17223.

Dua, D. and C. Graff (2017). UCI machine learning repository. <http://archive.ics.uci.edu/ml>.

Fanaee-T, H. and J. Gama (2014). Event labeling combining ensemble detectors and background knowledge. *Progress in Artificial Intelligence* 2(2), 113–127.

Friedman, J. H. (2001). Greedy function approximation: a gradient boosting machine. *Annals of statistics*, 1189–1232.

Frye, C., C. Rowat, and I. Feige (2020). Asymmetric Shapley values: incorporating causal knowledge into model-agnostic explainability. *Advances in Neural Information Processing Systems* 33, 1229–1239.

Grabisch, M. and M. Roubens (1999). An axiomatic approach to the concept of interaction among players in cooperative games. *International Journal of Game Theory* 28(4), 547–565.

Harris, C., R. Pymar, and C. Rowat (2022). Joint Shapley values: a measure of joint feature importance. In *International Conference on Learning Representations*.

Hiabu, M., E. Mammen, and J. T. Meyer (2020). Random planted forest: a directly interpretable tree ensemble. *arXiv preprint arXiv:2012.14563*.

Hooker, G. (2007). Generalized functional ANOVA diagnostics for high-dimensional functions of dependent variables. *Journal of Computational and Graphical Statistics* 16(3), 709–732.

Ittner, J., L. Bolikowski, K. Hemker, and R. Kennedy (2021). Feature synergy, redundancy, and independence in global model explanations using SHAP vector decomposition. *arXiv preprint arXiv:2107.12436*.

Janzing, D., L. Minorics, and P. Blöbaum (2020). Feature relevance quantification in explainable AI: A causal problem. In *International Conference on Artificial Intelligence and Statistics*, pp. 2907–2916. PMLR.

Kumar, I., C. Scheidegger, S. Venkatasubramanian, and S. Friedler (2021). Shapley residuals: Quantifying the limits of the Shapley value for explanations. *Advances in Neural Information Processing Systems* 34, 26598–26608.

Kumar, I. E., S. Venkatasubramanian, C. Scheidegger, and S. Friedler (2020). Problems with Shapley-value-based explanations as feature importance measures. In *Proceedings of the 37th International Conference on Machine Learning*, pp. 5491–5500. PMLR.

Lengerich, B., S. Tan, C.-H. Chang, G. Hooker, and R. Caruana (2020). Purifying interaction effects with the functional ANOVA: An efficient algorithm for recovering identifiable additive models. In *International Conference on Artificial Intelligence and Statistics*, pp. 2402–2412. PMLR.

Lipovetsky, S. and M. Conklin (2001). Analysis of regression in game theory approach. *Applied Stochastic Models in Business and Industry* 17(4), 319–330.

Lundberg, S. M., G. Erion, H. Chen, A. DeGrave, J. M. Prutkin, B. Nair, R. Katz, J. Himmelfarb, N. Bansal, and S.-I. Lee (2020). From local explanations to global understanding with explainable AI for trees. *Nature Machine Intelligence* 2(1), 56–67.

Lundberg, S. M. and S.-I. Lee (2017). A unified approach to interpreting model predictions. *Advances in Neural Information Processing Systems 30*.

Nembrini, S., I. R. König, and M. N. Wright (2018, 05). The revival of the Gini importance? *Bioinformatics 34*(21), 3711–3718.

Owen, G. (1972). Multilinear extensions of games. *Management Science 18*(5-part-2), 64–79.

Pearl, J. (2009). *Causality*. Cambridge University Press.

Ribeiro, M. T., S. Singh, and C. Guestrin (2016). "Why should I trust you?" explaining the predictions of any classifier. In *Proceedings of the 22nd ACM SIGKDD International Conference on Knowledge Discovery and Data Mining*, pp. 1135–1144.

Shapley, L. S. (1953). A value for n-person games, contributions to the theory of games, 2, 307–317.

Slack, D., S. Hilgard, E. Jia, S. Singh, and H. Lakkaraju (2020). Fooling LIME and SHAP: Adversarial attacks on post hoc explanation methods. In *Proceedings of the AAAI/ACM Conference on AI, Ethics, and Society*, pp. 180–186.

Stone, C. J. (1994). The use of polynomial splines and their tensor products in multivariate function estimation. *The Annals of Statistics 22*(1), 118–171.

Sundararajan, M., K. Dhamdhere, and A. Agarwal (2020). The Shapley Taylor interaction index. In *International Conference on Machine Learning*, pp. 9259–9268. PMLR.

Sundararajan, M. and A. Najmi (2020). The many Shapley values for model explanation. In *International Conference on Machine Learning*, pp. 9269–9278. PMLR.

Tsai, C.-P., C.-K. Yeh, and P. Ravikumar (2022). Faith-shap: The faithful shapley interaction index. *arXiv preprint arXiv:2203.00870*.

Williamson, B. and J. Feng (2020). Efficient nonparametric statistical inference on population feature importance using Shapley values. In *International Conference on Machine Learning*, pp. 10282–10291. PMLR.

Yeh, C.-K., K.-Y. Lee, F. Liu, and P. Ravikumar (2022). Threading the needle of on and off-manifold value functions for Shapley explanations. In *International Conference on Artificial Intelligence and Statistics*, pp. 1485–1502. PMLR.

Zhang, H., Y. Xie, L. Zheng, D. Zhang, and Q. Zhang (2021, May). Interpreting multivariate Shapley interactions in DNNs. *Proceedings of the AAAI Conference on Artificial Intelligence 35*(12), 10877–10886.

## A Shapley axioms

Given a function  $m$ , a point  $x_0$ , and a value function  $v$ , the Shapley axioms Shapley (1953) are

- **Efficiency:**  $m(x_0) = \phi_0 + \sum_{k=1}^d \phi_k(x_0)$ .
- **Symmetry:** Fix any  $k, l \in \{1, \dots, d\}, k \neq l$ . If  $v_{x_0}(S \cup k) = v_{x_0}(S \cup l)$ , for all  $S \subseteq \{1, \dots, d\} \setminus \{k, l\}$ , then  $\phi_k(x_0) = \phi_l(x_0)$
- **Dummy** If  $v_{x_0}(S \cup k) = v_{x_0}(S)$ , for all  $S \subseteq \{1, \dots, d\} \setminus \{k\}$ , then  $\phi_k = 0$
- **Linearity** If  $m(x_0) = m^1(x_0) + m^2(x_0)$ , then  $\phi_k(x_0) = \phi_k^1(x_0) + \phi_k^2(x_0)$ , where  $\phi^l$  is the explanation corresponding to the function  $m^l$ .

## B Lemmata and proofs

### B.1 Lemmata

**Lemma B.1.** The solution  $m_S^*$  described in theorem 2.1 can be re-written as

$$m_S^*(x_S) = \sum_{V \subseteq S} (-1)^{|S \setminus V|} \int m^{(0)}(x) p_{-V}(x_{-V}) dx_{-V},$$

where  $m^{(0)}(x) = \sum_S m_S^{(0)}(x_S)$ . In particular  $m_S^*$  does not depend on the particular identification of  $m^{(0)}$ .

*Proof.* We consider a fixed  $S \subseteq \{1, \dots, d\}$ . We will make use of the fact that for a set  $T \not\supseteq S$

$$\sum_{V \subseteq S} (-1)^{|S \setminus V|} \int m_T^{(0)}(x_T) p_{-V}(x_{-V}) dx_{-V} = 0, \quad (7)$$

and for a set  $T \subseteq \{1, \dots, d\}, T \supseteq S$

$$\{U : T \setminus S \subseteq U \subseteq T\} = \{T \setminus V : V \subseteq S\} \quad (8)$$

Combining (7)–(8), we get

$$\begin{aligned} & \sum_{V \subseteq S} (-1)^{|S \setminus V|} \int m^{(0)}(x) p_{-V}(x_{-V}) dx_{-V} \\ &= \sum_{T \subseteq \{1, \dots, d\}} \sum_{V \subseteq S} (-1)^{|S \setminus V|} \int m_T^{(0)}(x_T) p_{-V}(x_{-V}) dx_{-V} \\ &= \sum_{T \supseteq S} \sum_{V \subseteq S} (-1)^{|S| - |V|} \int m_T^{(0)}(x_T) p_{T \setminus V}(x_{-T \setminus V}) dx_{T \setminus V} \\ &= \sum_{T \supseteq S} \sum_{T \setminus S \subseteq U \subseteq T} (-1)^{|S| - |T \setminus U|} \int m_T^{(0)}(x_T) p_U(x_U) dx_U. \end{aligned}$$

It is left to show (7)–(8). Equation (8) follows from straight forward calculations. To see 7, note

$$\begin{aligned}
& \sum_{V \subseteq S} (-1)^{|S \setminus V|} \int m_T^{(0)}(x_T) p_{-V}(x_{-V}) dx_{-V} \\
&= \sum_{U \subseteq S \cap T} \sum_{W \subseteq S \setminus T} (-1)^{|S \setminus \{W \cup U\}|} \int m_T^{(0)}(x_T) p_{-\{U \cup W\}}(x_{-\{U \cup W\}}) dx_{-\{U \cup W\}} \\
&= \sum_{U \subseteq S \cap T} \int m_T^{(0)}(x_T) p_{-U}(x_{-U}) dx_{-U} \sum_{W \subseteq S \setminus T} (-1)^{|S \setminus \{W \cup U\}|} \\
&= \sum_{U \subseteq S \cap T} \int m_T^{(0)}(x_T) p_{-U}(x_{-U}) dx_{-U} \left( \sum_{W \subseteq S \setminus T, |W|=\text{odd}} (-1)^{|S \setminus U|-1} + \sum_{W \subseteq S \setminus T, |W|=\text{even}} (-1)^{|S \setminus U|} \right) \\
&= 0,
\end{aligned}$$

where the last equality follows from the fact that every non-empty set has an equal number of odd and even subsets.  $\square$

**Lemma B.2** (Shapley (1953)). For every  $U \subseteq \{1, \dots, d\}$ ,

$$\int m(x) p_{-U}(x_{-U}) dx_{-U} = \sum_{T \subseteq U} m_T^*(x_T)$$

*Proof.*

$$\begin{aligned}
\sum_{T \subseteq U} m_T(x_T) &= \sum_{T \subseteq U} \sum_{V \subseteq T} (-1)^{|T \setminus V|} \int m^{(0)}(x) p_{-V}(x_{-V}) dx_{-V} \\
&= \sum_{V \subseteq U} \int m^{(0)}(x) p_{-V}(x_{-V}) dx_{-V} \sum_{S \subseteq \{1, \dots, |U \setminus V|\}} (-1)^{|S|} \\
&\quad + \int m^{(0)}(x) p_{-U}(x_{-U}) \\
&= \int m^{(0)}(x) p_{-U}(x_{-U}),
\end{aligned}$$

where the last equation follows from  $\sum_{S \subseteq \{1, \dots, |U \setminus V|\}} (-1)^{|S|} = 0$ , noting that a non-empty set has an equal number of subsets with an odd number of elements as subsets with an even number of elements.  $\square$

## B.2 Proofs

*Proof of Corollary 2.3.* This proof is analogue to the proof of Lemma 3.1 in Shapley (1953). From B.2, We have  $\int m(x) p_{-U}(x_{-U}) dx_{-U} = \sum_{T \subseteq U} m_T^*(x_T)$ . Hence the game  $m$  with value function

$$v_m(U) = \int m(x) p_{-U}(x_{-U}) dx_{-U}$$

equals the game  $m^*$  with value function

$$v_{m^*}(U) = \sum_{S \subseteq \{1, \dots, d\}} m_S^*(x_S) \delta_S(U), \quad \delta_S(U) = 1(S \subseteq U).$$

We now concentrate on the function  $m_S^*$  with value function  $m_S^*(x_S) \delta_S(U)$ . We will show that for every non-empty  $S \subseteq \{1, \dots, d\}$ ,

$$\phi_k(x, m_S^*(x_S) \delta_S(U)) = 1(k \in S) |S|^{-1} m_S^*(x_S). \quad (9)$$

Here,  $\phi_k(x, v)$  denotes the Shapley value for feature  $k$  at point  $x$  in a game with value function  $v$ . The proof is then completed by the additivity axiom, together with

$$\phi_k(x, m_\emptyset^* \delta_\emptyset(U)) = \begin{cases} m_\emptyset^*, & k = 0, \\ 0 & \text{else.} \end{cases}$$

The last statement follows from the dummy axiom. To show (9), let's assume that  $j, k \in S$ . Then for every  $U \subseteq \{1, \dots, d\}$ ,  $m_S^*(x_S) \delta_S(U \cup j) = m_S^*(x_S) \delta_S(U \cup k)$ , which, by the symmetry axiom, implies

$$\phi_j(x, m_S^*(x_S) \delta_S(U)) = \phi_k(x, m_S^*(x_S) \delta_S(U)).$$

Additionally, for  $k \notin S$ , we have  $\phi_j(x, m_S^*(x_S) \delta_S(U)) = 0$ , by the dummy axiom. Hence we conclude (9) by applying (4).  $\square$

*Proof of Theorem 2.2.* Lemma B.2 implies that  $m^*$  is a solution. To see this, for  $S \subseteq \{1, \dots, d\}$ , consider the following decomposition of  $\int m^*(x) p_S(x_S) dx_S$

$$\int m^*(x) p_S(x_S) dx_S = \sum_{T \cap S \neq \emptyset} \int m_T^*(x_T) p_S(x_S) dx_S + \sum_{T \cap S = \emptyset} m_T^*(x_T).$$

Using Lemma B.2, we have

$$\int m^*(x) p_S(x_S) dx_S = \sum_{T \subseteq S^c} m_T^*(x_T) = \sum_{T \cap S = \emptyset} m_T^*(x_T),$$

which with the previous statement implies that  $m^*$  is a solution:

$$\sum_{T \cap S \neq \emptyset} \int m_T^*(x_T) p_S(x_S) dx_S = 0.$$

It is left to show that the solution is unique. Note that for every  $S \subseteq \{1, \dots, d\}$

$$\sum_T \int m_T(x_T) p_S(x_S) dx_S = \sum_{T \cap S = \emptyset} m_T(x_T) + \sum_{T \cap S \neq \emptyset} \int m_T(x_T) p_S(x_S) dx_S.$$

Hence, condition (2) is equivalent to

$$\sum_T \int m_T(x_T) p_S(x_S) dx_S = \sum_{T \cap S = \emptyset} m_T(x_T). \quad (10)$$

Now assume that there are two set of functions  $m^\circ$  and  $m^*$  that satisfy (2) with  $\sum_S m_S^\circ = \sum_S m_S^*$ . From (10), it follows that for all  $S \subseteq \{1, \dots, d\}$

$$\sum_{T \cap S = \emptyset} m_T^\circ(x_T) = \sum_{T \cap S = \emptyset} m_T^*(x_T),$$

implying  $m_T^\circ(x_T) = m_T^*(x_T)$  for all  $T \subseteq \{1, \dots, d\}$ .  $\square$

## C Connecting a general global expansion to SHAP values

If a regression or classification function  $m$  is not identified via (2), then calculating SHAP values from such a decomposition leads to lengthy and non-trivial expressions. Here, we show how the terms up to dimension three in a general non-identified decomposition enter into a SHAP value. The following formula follows from straight forward calculations using (4).

For  $v_x(S) = \int m(x)p_{-S}(x_{-S})dx_{-S}$ , we get

$$\begin{aligned}
\phi_1(x_0) = & m_1(x_1) - E[m_1(X_1)] \\
& + \frac{1}{2} \left\{ \sum_{j \neq 1} m_{1j}(x_1, x_j) - E[m_{1j}(X_1, X_j)] \right. \\
& \quad \left. + \sum_{j \neq 1} E[m_{1j}(x_1, X_j)] - E[m_{1j}(X_1, x_j)] \right\} \\
& + \frac{1}{3} \left\{ \sum_{j, k \neq 1, j < k} m_{1jk}(x_1, x_j, x_k) - E[m_{1jk}(X_1, X_j, X_k)] \right. \\
& \quad + \sum_{j, k \neq 1, j < k} E[m_{1jk}(x_1, X_j, X_k)] - E[m_{1jk}(X_1, x_j, x_k)] \\
& \quad + \frac{1}{2} \sum_{j, k \neq 1, j < k} E[m_{1jk}(x_1, X_j, x_k)] - E[m_{1jk}(X_1, x_j, X_k)] \\
& \quad + \frac{1}{2} \sum_{j, k \neq 1, j < k} E[m_{1jk}(x_1, x_j, X_k)] - E[m_{1jk}(X_1, X_j, x_k)] \right\} \\
& + \frac{1}{4} \left\{ \sum_{j, k, l \neq 1, j < k < l} m_{1jkl}(x_1, x_j, x_k, x_l) - E[m_{1jkl}(X_1, X_j, X_k, X_l)] \right. \\
& \quad + \sum_{j, k \neq 1, j < k < l} E[m_{1jk}(x_1, X_j, X_k, X_l)] - E[m_{1jk}(X_1, x_j, x_k, x_l)] \\
& \quad + \frac{1}{2} \sum_{j, k \neq 1, j < k < l} E[m_{1jk}(x_1, x_j, X_k, X_l)] - E[m_{1jk}(X_1, X_j, x_k, x_l)] \\
& \quad + \frac{1}{2} \sum_{j, k \neq 1, j < k < l} E[m_{1jk}(x_1, X_j, x_k, X_l)] - E[m_{1jk}(X_1, x_j, X_k, x_l)] \\
& \quad + \frac{1}{2} \sum_{j, k \neq 1, j < k < l} E[m_{1jk}(x_1, X_j, X_k, x_l)] - E[m_{1jk}(X_1, x_j, x_k, X_l)] \\
& \quad + \frac{1}{3} \sum_{j, k \neq 1, j < k < l} E[m_{1jk}(x_1, x_j, x_k, X_l)] - E[m_{1jk}(X_1, X_j, X_k, x_l)] \\
& \quad + \frac{1}{3} \sum_{j, k \neq 1, j < k < l} E[m_{1jk}(x_1, x_j, X_k, x_l)] - E[m_{1jk}(X_1, X_j, x_k, X_l)] \\
& \quad + \left. \frac{1}{3} \sum_{j, k \neq 1, j < k < l} E[m_{1jk}(x_1, X_j, x_k, x_l)] - E[m_{1jk}(X_1, x_j, X_k, X_l)] \right\} \\
& \quad \dots
\end{aligned}$$

## D Calculating the functional decomposition of SHAP values from low-dimensional tree structures

Our proposed decomposition can be calculated from tree-based models by directly applying Theorem 2.1. Inspired by Lundberg et al. (2020), we first describe naïve algorithms for *xgboost* and *random planted forest* models and then describe an improved algorithm for *xgboost* that only needs a single recursion through each tree.

### D.1 Naïve xgboost algorithm

For all subsets of features  $S \subseteq \{1, \dots, d\}$ , we calculate the decomposition  $\hat{m}_S(x_i)$  for all observations of interest  $x_i \in \mathbf{X}$  recursively for each tree with features  $T$  by considering all subsets  $U, T$  with  $T \setminus S \subseteq U \subseteq T$ . In each node of a tree, if the node is a leaf node we return it's prediction (e.g. the mean in CART-like trees). For internal (non-leaf) nodes, the procedure depends on whether the feature used for splitting in the node is in the subset  $U$  or not. If the feature is in the subset  $U$ , we continue in both the left and right children nodes, each weighted by the coverage, i.e. the proportion of training observations going left and right, respectively. If the feature is not in the subset  $U$ , we apply the splitting criterion of the node and continue with the respective node selected by the splitting procedure for observation  $x_i$ . See Algorithm 1 for the full algorithm in pseudo code.

---

**Algorithm 1** NAÏVE XGBOOST ALGORITHM

---

**Procedure:** DECOMPOSE( $\mathbf{X}, \hat{m}(x)$ )  
**Input:** Dataset to be explained  $\mathbf{X} \in \mathbb{R}^{n \times d}$ , tree-based model  $\hat{m}(x)$  with  $B$  trees  
**Output:** Components  $\hat{m}_S(x_i)$  for all  $S \subseteq \{1, \dots, d\}$  and  $x_i \in \mathbf{X}$

**for**  $i \in 1, \dots, n$  **do**

- for**  $S \subseteq \{1, \dots, d\}$  **do**
- $\hat{m}_S(x_i) \leftarrow 0$
- for** tree  $\in \{1, \dots, B\}$  **do**
- if**  $T \supseteq S$  **then**
- for**  $U : T \setminus S \subseteq U \subseteq T$  **do**
- $\hat{m}_S(x_i) \leftarrow \hat{m}_S(x_i) + (-1)^{|S|-|T \setminus U|} \text{RECURSE(tree, } U, x_i, 0)$
- end for**
- end if**
- end for**
- end for**

**Return:**  $\hat{m}_S$

**Procedure:** RECURSE(tree,  $U, x_i, \text{node}$ )  
**Input:** Tree ID (tree), subset  $U$ , data point  $x_i$ , node ID (node)  
**Output:** Coverage-weighted prediction

**if** ISLEAF(node) **then**

- Return:** PREDICTION(node)

**else**

- $j \leftarrow \text{SPLIT-FEATURE}(\text{node})$
- if**  $j \in U$  **then**
- $C_{\text{left}} \leftarrow \text{COVERAGE}(\text{left-node})$
- $C_{\text{right}} \leftarrow \text{COVERAGE}(\text{right-node})$
- Return:**  $C_{\text{left}} \text{RECURSE(tree, } U, x_i, \text{left-node}) + C_{\text{right}} \text{RECURSE(tree, } U, x_i, \text{right-node})$

**else**

- if**  $x_i^j \leq \text{SPLIT-VALUE}(\text{node})$  **then**
- Return:** RECURSE(tree,  $U, x_i, \text{left-node}$ )
- else**
- Return:** RECURSE(tree,  $U, x_i, \text{right-node}$ )
- end if**

**end if**

**end if**

---

## D.2 Naïve random planted forest algorithm

For the random planted forest algorithm (rpf), we use a different approach. By slightly altering the representation of an rpf in Hiabu et al. (2020), the result of

an rpf is given by a set

$$\hat{m}^{(0)} = \{\hat{m}_{S,b}^{(0)} | S \subseteq \{1, \dots, d\}, b \in \{1, \dots, B\}\},$$

where each estimator  $\hat{m}_{S,b}^{(0)}$  can be represented by a finite partition defined by an  $|S|$ -dimensional grid (leaves) and corresponding values. Thus, we start with

- a grid  $G_k = \{x_{k,1}, \dots, x_{k,t_k}\}$  for each coordinate  $k \in \{1, \dots, d\}$ ,
- for each  $S \subseteq \{1, \dots, d\}, b \in \{1, \dots, B\}$  an array representing the value of  $\hat{m}_{S,b}^{(0)}(x)$  for each coordinate  $x \in \times_{k \in S} G_k$ . Here  $x$  is considered to be the bottom left corner of a hyperrectangle.

Note that every tree-based algorithm can be described in such a manner. Given an estimator  $\hat{p}_S$  and using this representation, directly calculating (3) is simple, where for each combination of sets  $U, T \subseteq \{1, \dots, d\}$  with  $U \subseteq T$ , we only need to calculate the term  $\int \hat{m}_{T,b}^{(0)}(x_T) \hat{p}_U(x_U) dx_U$  once and then add/subtract it to the correct estimators  $\hat{m}_S^*$ . See Algorithm 2 for the full algorithm in pseudo code.

---

**Algorithm 2** NAÏVE RPF ALGORITHM

---

**Procedure:** DECOMPOSE( $\mathbf{X}, \hat{m}(x)$ )

**Input:** Dataset to be explained  $\mathbf{X} \in \mathbb{R}^{n \times d}$ , tree-based model with initial decomposition  $\hat{m}_{S,b}^{(0)}(x)$  for  $S \subseteq \{1, \dots, d\}$  and trees  $b = \{1, \dots, B\}$ , estimator  $\hat{p}_S$

**Output:** Components  $\hat{m}_S(x_i)$  for all  $S \subseteq \{1, \dots, d\}$  and  $x_i \in \mathbf{X}$

**for**  $i \in 1, \dots, n$  **do**

**for**  $S \subseteq \{1, \dots, d\}$  **do**

$\hat{m}_S(x_i) \leftarrow 0$

**end for**

**for**  $b \in \{1, \dots, B\}$  **do**

**for**  $T \subseteq \{1, \dots, d\}$  **do**

**for**  $U \subseteq T$  **do**

$\text{update}_{T,U} \leftarrow \int \hat{m}_{T,b}^{(0)}(x_{i,T \setminus U}, x_U) \hat{p}_U(x_U) dx_U$

**for**  $S : T \setminus S \subseteq U, S \subseteq T$  **do**

$\hat{m}_S(x_i) \leftarrow \hat{m}_S(x_i) + (-1)^{|S| - |T \setminus U|} \text{update}_{T,U}$

**end for**

**end for**

**end for**

**end for**

$\hat{m}_S(x_i) \leftarrow \hat{m}_S(x_i) / B$

**end for**

**Return:**  $\hat{m}_S$

---

For the calculation of an estimator  $\hat{p}_S$  in our simulations we used the following. For each  $S \subseteq \{1, \dots, d\}$ , let  $a_S(x)$  be the number of data points residing in the

hyperrectangle with bottom left corner  $x$  for each coordinate  $x \in \times_{k \in S} G_k$ . For  $|S|$ -dimensional  $y$  we then set

$$\hat{p}_S(y) = \frac{a_S(x_y)}{\sum_{x \in \times_{k \in S} G_k} a_S(x)} \frac{1}{\text{vol}(x)},$$

where  $x_y$  is the coordinate of the bottom left corner of the hyperrectangle which includes  $y$  and  $\text{vol}(x)$  is the volume of the hyperrectangle corresponding to  $x$ . Using this estimator, the updating function in the algorithm simplifies to

$$\text{update}_{T,U} = \sum_{x_U \in \times_{k \in U} G_k} \hat{m}_{T,b}^{(0)}(x_{i,T \setminus U}, x_U) \hat{p}_U(x_U).$$

### D.3 Improved xgboost algorithm

To improve the algorithm described in Section D.1 and Algorithm 1, we pre-calculate the contribution of each tree for all  $n$  observations and tree-subsets  $T$  in a single recursive procedure by filling an  $n \times 2^D$  matrix, where  $D$  is the tree depth. In a second step, we just have to sum these contributions with the corresponding sign (see Theorem 2.1).

## E Experiments with random planted forest

This section shows the simulation results when using the *random planted forest algorithm* as an estimation procedure. First of all, the results considering the motivating example from Section 1.1 are given in Figure 6. The following subsections include the results of experiments which were discussed in Section 4.

### E.1 Global explanations

Figure 7 includes the results discussed in Section 4.1 when considering the *random planted forest algorithm* instead of *xgboost*.

### E.2 Feature importance

Figure 8 includes the results discussed in Section 4.2 when considering the *random planted forest algorithm* instead of *xgboost*.

### E.3 Post-hoc feature removal

Figure 9 includes the results discussed in Section 4.3 when considering the *random planted forest algorithm* instead of *xgboost*.

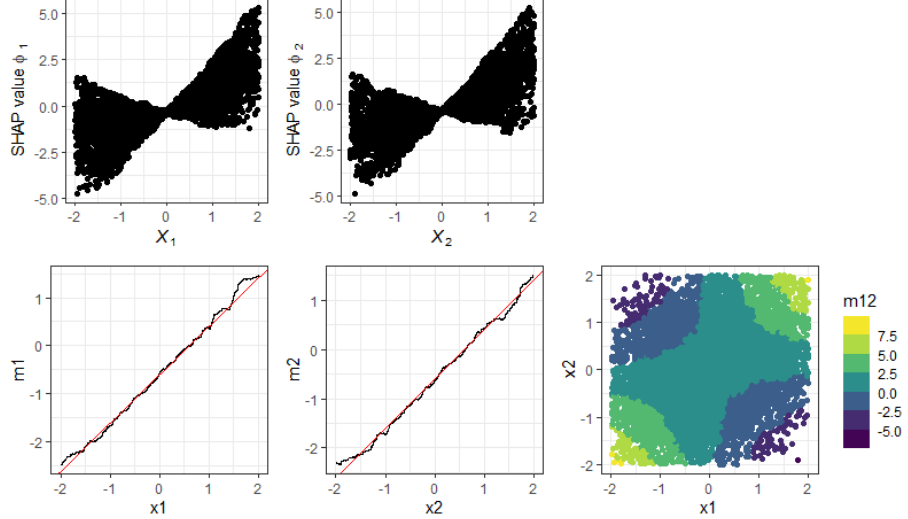


Figure 6: Simple example. SHAP values (top row) and functional decomposition (bottom row) of a *random planted forest* model of the function  $m(x_1, x_2) = x_1 + x_2 + 2x_1x_2$ . The red lines in the bottom row represent the SHAP values of the true function.

## F Relationship of global explanation to partial dependence plots

Given an estimator  $\hat{m}$  and a target subset  $S \subset \{1, \dots, d\}$ , the partial dependence plot Friedman (2001),  $\xi_S$ , is defined as

$$\xi_S(x_S) = \int \hat{m}(x)p_{-S}(x_{-S})dx_{-S}.$$

It is straight forward to verify that partial dependence plots are linked to a functional decomposition  $\{\hat{m}_S^*\}$  identified via (2) through

$$\xi_S = \sum_{U \subseteq S} \hat{m}_U^*.$$

## G Computing environment

A 64-bit Linux platform running Ubuntu 20.04 with an AMD Ryzen Threadripper 3960X (24 cores, 48 threads) CPU and 256 GByte RAM was used for all computations with R version 4.1.2.

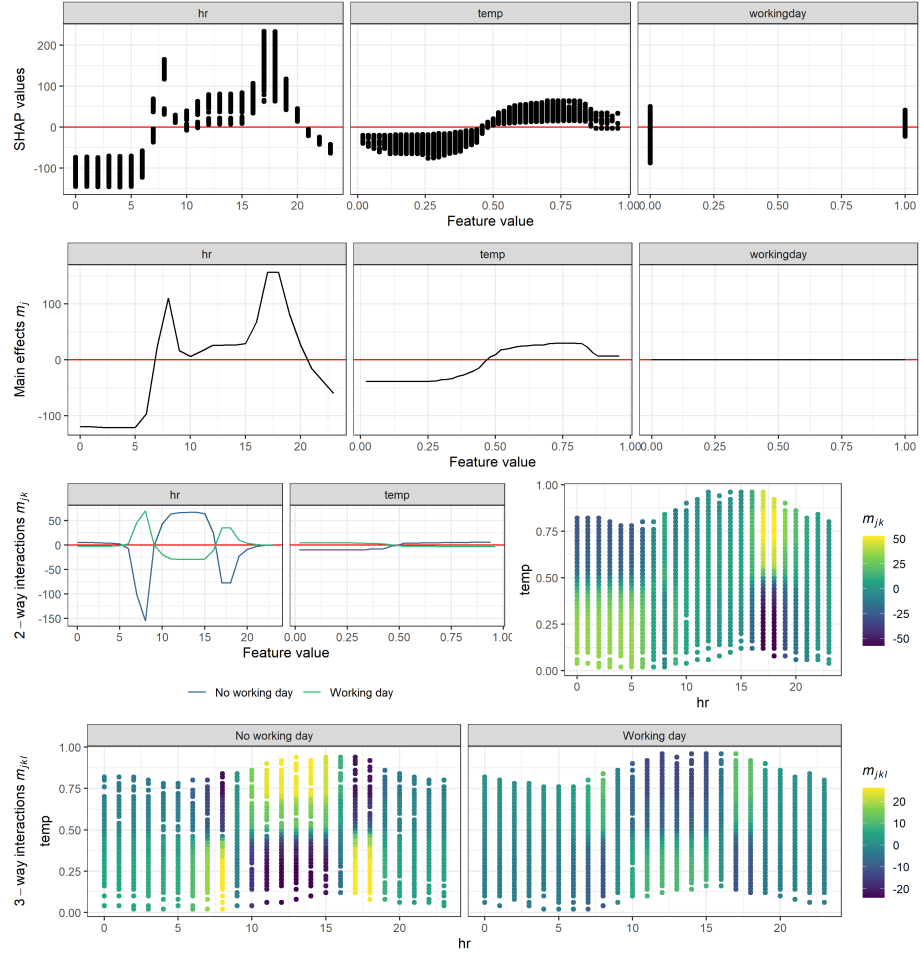


Figure 7: Bike sharing example (*random planted forest*). SHAP values (top row), main effects (second row), 2-way interactions (third row) and 3-way interactions (bottom row) of the features *hour of the day* (hr, 0-24 full hours), *Temperature* (temp, normalized to 0-1) and *working day* (workingday, 0=no, 1=yes) of the bike sharing data.

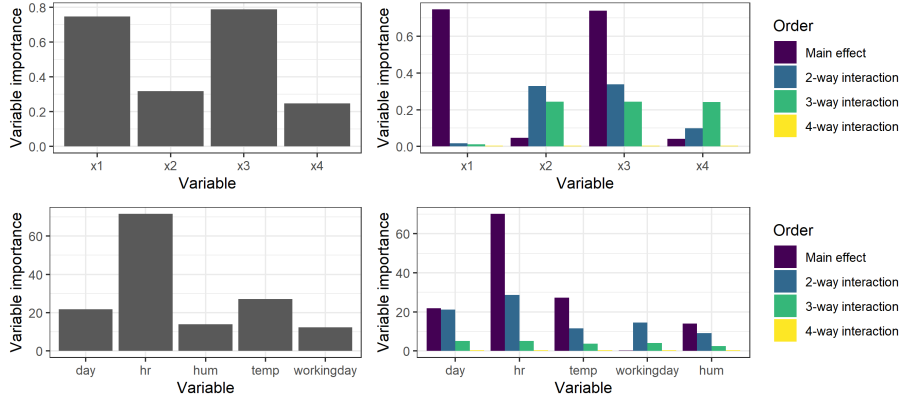


Figure 8: Feature importance (*random planted forest*) for the function  $m(x) = x_1 + x_3 + x_2x_3 - 2x_2x_3x_4$  (top row) and the bike sharing data from Section 4.1 (bottom row) based on SHAP values (left column) and our functional decomposition separately for main effects and interactions of different orders (right column).

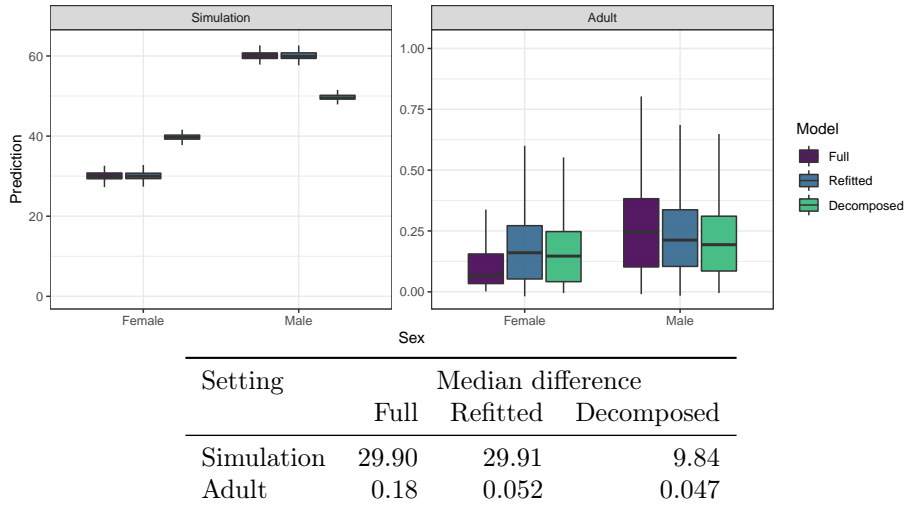


Figure 9: Post-hoc feature removal (*random planted forest*). Predictions in a simulation (left) and the *adult* dataset for males and females of the full model, a refitted model without the protected feature *sex* and a decomposed model where the feature *sex* was removed post-hoc. The table below shows the median differences between females and males for the three models.